

Trends in bulk electron-structural features of early transition-metal carbides

Aleksandra Vojvodic^{1,*} and Carlo Ruberto¹

¹*Department of Applied Physics, Chalmers University of Technology, SE-412 96 Göteborg, Sweden*

(Dated: January 15, 2021)

A detailed and systematic density-functional theory (DFT) study of a series of early transition-metal carbides (TMC's) in the NaCl structure is presented. The focus is on the trends in the electronic structure and nature of bonding, which are essential for the understanding of the reactivity of TMC's. The employed approach is based on a thorough complementary analysis of the electron density differences, the density of states (DOS), the band structure, and the real-space wave functions to gain insight into the bonding of this class of materials and get a more detailed picture of it than previously achieved, as the trend study allows for a systematic identification of the bond character along the different bands. Our approach confirms the presence of both the well-known TM–C and TM–TM bonds and, more importantly, it shows the existence and significance of direct C–C bonds in all investigated TMC's, which are frequently neglected but have been recently identified in some cases [Solid State Commun. **121**, 411 (2002); Phys. Rev. B **75**, 235438 (2007)]. New information on the spatial extent of the bonds, their k -space location within the band structure, and their importance for the bulk cohesion is provided. Trends in covalency and ionicity are presented. The resulting electron-structural trends are analyzed and discussed within a two-level model.

PACS numbers: 71.,71.20.-b,71.15.Mb,71.15.Nc

I. INTRODUCTION

An extensive study of the reactivity of the transition-metal carbide and nitride (TMX) surfaces is being performed with the density-functional theory (DFT).^{1–6} It is aimed at an understanding of reactivity from fundamental principles, similar to the one available today for pure metal surfaces.⁷ Due to the intimate relation between bulk and surface electronic structures, a careful mapping of trends in the bulk electronic structure is essential for the overall purpose to understand the trends in reactivity of the transition-metal carbides (TMC's). Therefore, a bulk background focusing on the trends in electronic structure and nature of bonding in the early transition-metal carbides (TMC) is here provided.

The relevance of the results is, however, broader, as the bulk TMX's are also interesting by themselves, having such properties as extremely high melting point, ultrahardness, and metallic conductivity.^{8,9} As a consequence, the importance of the electronic-structure trends for atomic structure and stability is also analyzed.

The bulk TMX's have been studied experimentally and theoretically with a large number of techniques.^{1,10–24} Already the early studies agree on the fact that the bonding in these compounds involves simultaneous contributions from metallic, covalent, and ionic bonding.¹¹ The main electronic-structure properties are related to (i) the direction and amount of charge transfer between the TM and X atoms, responsible for the ionicity of the material, and (ii) the modifying effect on the metal d band upon the carbide/nitride formation, responsible for the formation of hybridized bonding and antibonding pd states. The decreasing stability of the TMC's in NaCl structure from left to right along a period in the periodic table has been explained as arising from the successive filling of the antibonding TMd – Cp states in a rigid-band model.^{13,15,20}

Recently, the contributions to the cohesive energy from the TM–C, TM–TM, and C–C bonds, respectively, have been approximately determined quantitatively by a two-sublattice model of the NaCl structure based on DFT calculations.¹⁴ These results confirm the dominance of the TM–C bond (strongest for TiC) and the importance of the TM–TM bond (strongest for VC). In addition, they show that direct C–C interactions cannot be neglected in some of the considered TMC's (from CrC to NiC along period 4 in the periodic table). The used model, however, falls short of explaining such results from the calculated electronic structures.

Our systematic DFT investigation is performed on a number of non-magnetic early TMC's. Complementary electronic-structure analysis tools are employed in a joined way to obtain detailed information of the bond character: valence-electron density differences, Bader charge analyses, band structures, projected densities of states (DOS), and real-space wave functions. Key bulk properties are calculated, compared with earlier studies, and analyzed on the basis of the obtained knowledge of the electronic structure. The studied subgroup of TMC's (Fig. 1) is chosen to allow a monitoring of trends with respect to the constituent transition metals (TM) along both period and group within the periodic table. Also, some of these TMC's are widely used in applications. We argue that the subgroup is large enough to pick up the important trends.

Many TMC's crystallize in the sodium chloride structure, either as stable, including ScC (at normal pressures), TiC, VC, ZrC, NbC, and TaC, or metastable compounds, such as δ -MoC and WC. The choice of the TMC's in the NaCl structure is natural for our calculations since the number of varying parameters should be kept small when performing a trend study to allow for an identification of the important electronic factors.

per \ grp	IIIb	IVb	Vb	
3d	ScC	TiC	VC	
4d		ZrC	NbC	MoC
5d			TaC	WC

FIG. 1: The early transition-metal carbides under investigation, organized according to their parent-metal position in the periodic table.

The Paper is organized as follows. First, the computational details are summarized in Sec. II. Then, in Sec. III, the results from our calculations are presented and the obtained trends analyzed, including: atomic geometry and stability (Sec. III A), electron density and charge transfer (Sec. III B) and detailed electronic structure (Sec. III C). In Sec. IV, these trends and the nature of bonding in the TMC's are summarized, discussed, and related. The main conclusions of our study are summarized in Sec. V.

II. COMPUTATIONAL DETAILS

The calculations presented in this paper are performed within the well-established DFT formalism using the plane-wave pseudopotential code Dacapo.²⁵ The ion-electron interaction is treated with Vanderbilt ultrasoft pseudopotentials.²⁶ The exchange-correlation energy is included by the generalized gradient approximation (GGA), using the PW91 functional.²⁷ All the bulk calculations are performed with a Monkhorst-Pack sampling²⁸ of $8 \times 8 \times 8$ special k -points and a cutoff energy for the plane-wave expansion of 400 eV. The similarities and differences in the nature of bonding in the considered TMC's are studied with the following electron-structure analysis tools: electronic density differences, Bader charge analyses,^{30,31} band structure diagrams, atom-projected local DOS's, and Kohn-Sham wave functions. The Bader analysis is a charge-localization analysis that is able to give quantitative information of the electron localization around different ions. The scheme used here is based on the approach described in Refs. 30 and 31.

III. RESULTS AND ANALYSIS

A. Geometry and Stability

In Table I and Fig. 2 we present the calculated lattice parameters, bulk moduli, and cohesive energies, together with the available experimental data. The lattice parameters and the bulk moduli are obtained with a Muraghan equation of state²⁹ and the cohesive energies are

TABLE I: Calculated lattice parameters (a_0), cohesive energies (E_{coh}), bulk moduli (B_0), and Bader charge transfers from TM to C atoms (Bader). The corresponding experimental values are given in parentheses. The calculated E_{coh} values are defined by Eq. (1).

TMC	a_0 (Å)	E_{coh} (eV/unit cell)	B_0 (GPa)	Bader (e /atom)
ScC	4.684 (4.637) ^a	12.39 (12.74) ^d	148 (-)	1.54
TiC	4.332 (4.325) ^b	14.90 (14.32) ^d	242 (232-390) ^c	1.49
VC	4.164 (4.163) ^b	13.88 (13.88) ^d	290 (308-390) ^c	1.41
ZrC	4.702 (4.691) ^b	15.93 (15.86) ^e	258 (159-224) ^c	1.70
NbC	4.492 (4.454) ^b	15.83 (16.52) ^e	293 (296-330) ^c	1.64
δ -MoC	4.450 (4.270) ^e	13.11 (14.45) ^e	319 (-)	1.97
TaC	4.479 (4.453) ^b	17.34 (17.12) ^f	321 (214-414) ^c	1.94
WC	4.382 (-)	15.67 (16.49) ^f	357 (-)	1.60

^aRef. 24.

^bRef. 32.

^cRefs. 9 and 23.

^dRef. 17.

^eRef. 18.

^fRef. 19.

calculated as

$$E_{\text{coh}} = E_{\text{solid}} - \sum_{\text{atoms}} E_{\text{atom}}^{\text{isolated}}. \quad (1)$$

There is good agreement between calculated and experimental values. For the lattice parameters the deviations are smaller than 1%. Our calculated lattice constants are also in quantitative agreement with other published theoretical results, obtained with both the PW91 and the RPBE GGA functionals.²³

For both the cohesive energies and the bulk moduli the deviations from experiments are larger. Still, our results agree well with other theoretical values.²²⁻²⁴ The deviations from experiments can be understood from the fact that in reality the TMC's often occur as substoichiometric phases, with strongly varying amounts of carbon vacancies. It is known that several bulk properties depend strongly on such defects.^{21,33}

The trends in lattice parameters can be understood qualitatively by plotting them against empirical covalent³⁴ and ionic³⁵ radii (Fig. 3). The overall linear correlations indicate that the bonding in the TMC's contains both covalent and ionic effects. This iono-covalent mixture agrees with earlier studies¹¹ and is examined in more detail in our analysis of the electronic structure below.

The cohesive energies increase monotonically down a group in the periodic table. Along each period, they exhibit a maximum for group IV. These trends agree with the experimental values (see Table I). As will be argued below, these trends can be understood from the trends of the bulk electronic structure.

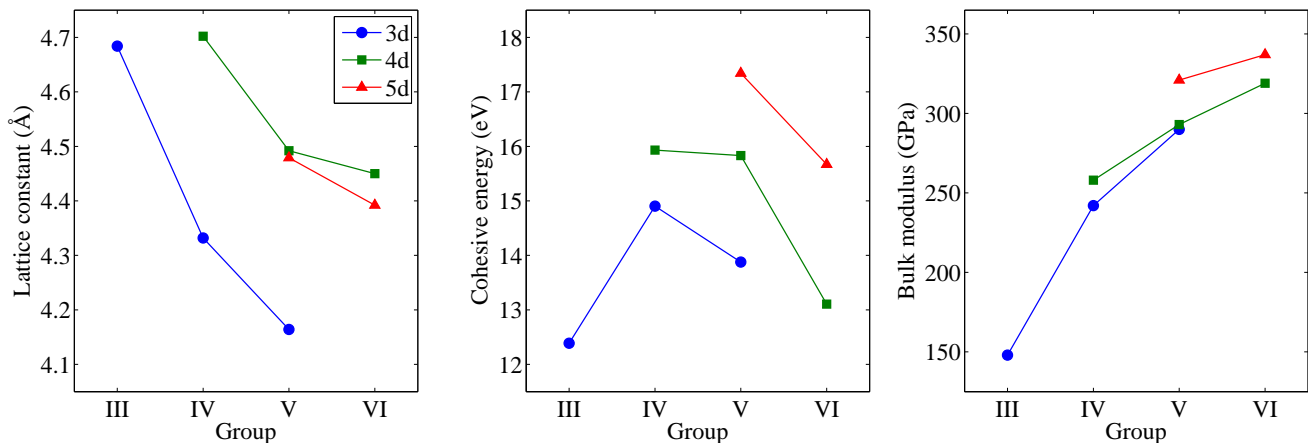


FIG. 2: Variations of, from left to right, the lattice parameters, the cohesive energies, and the bulk moduli of the investigated 3d, 4d, and 5d TMC's as a function of the group number of their parent transition metals.

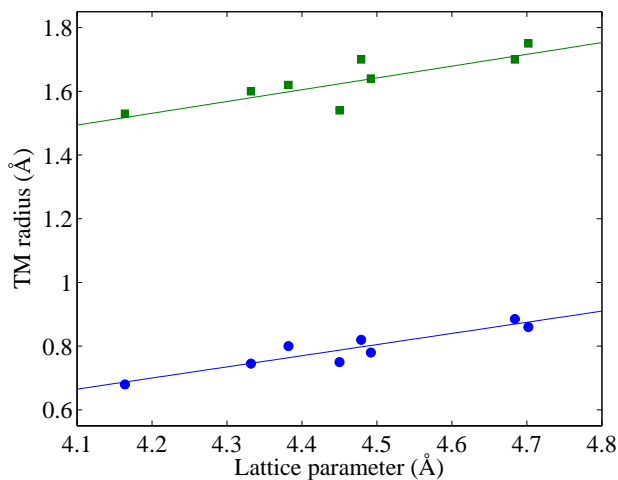


FIG. 3: The linear correlations of the TMC lattice parameters with the covalent radii³⁴ (squares) and with the ionic radii³⁵ (circles) of the parent transition metals.

B. Valence Electron Density and Charge Transfer

Three-dimensional contour plots of the differences between the valence electron densities in the bulk TMC's and the electron densities of free TM and C atoms are shown in Fig. 4 for the considered TMC's. The changes in the distribution of the valence electrons upon bond creation in the bulk TMC's reveal (i) a partially ionic character of the bond, seen as quite localized electron clouds (orange-red regions) around the C atoms, indicating a charge transfer from TM to C, and (ii) covalent TM-C σ bonds, seen as a localization of charge (orange) in the region in between the TM and C atoms.

Our Bader analysis results presented in Table I confirm that the TMC's are partly ionic compounds. Charge is transferred from TM to C for all considered compounds,

as expected from the higher electronegativity of C. This direction of the charge transfer is confirmed experimentally by the near-edge X-ray absorption fine structure (NEXAFS) technique.³⁶

The covalent nature of the bonding is most evident in TiC and VC, as shown by the charge-difference contours (Fig. 4) and by the lower Bader charge transfer for these compounds. In general, the Bader charge trends indicate (i) an increase in covalency and a decrease in ionicity (an exception is the metastable δ -MoC), when moving from left to right along a period, and (ii) a decrease in covalency and an increase in ionicity down a group.

All of the considered carbides except MoC and WC are stable in the NaCl structure. The electron-density difference alone cannot explain why this is the case. To gain an understanding of the structure change of WC other methods must be employed, including the ones in the next Section.

C. Electronic Structure and Nature of Bonding

1. General Features

Calculated total and atom-projected DOS's and band structures for the considered bulk TMC's are shown in Figs. 5 and 6, respectively. Furthermore, complementary information about the bond character for different bands and k points is obtained by investigating the real-space Kohn-Sham wave functions in detail. Such an analysis is performed for all the TMC's. The results are presented in Fig. 6 and a representative selection of the different bond types is illustrated in Fig. 7.

The overall electronic structure is similar for all considered TMC's and is characterized by (i) a deeply bound lower valence band (LVB) with C 2s states and a very small amount of TM d states (not shown in the DOS figures for all the TMC's in the given energy interval); (ii)

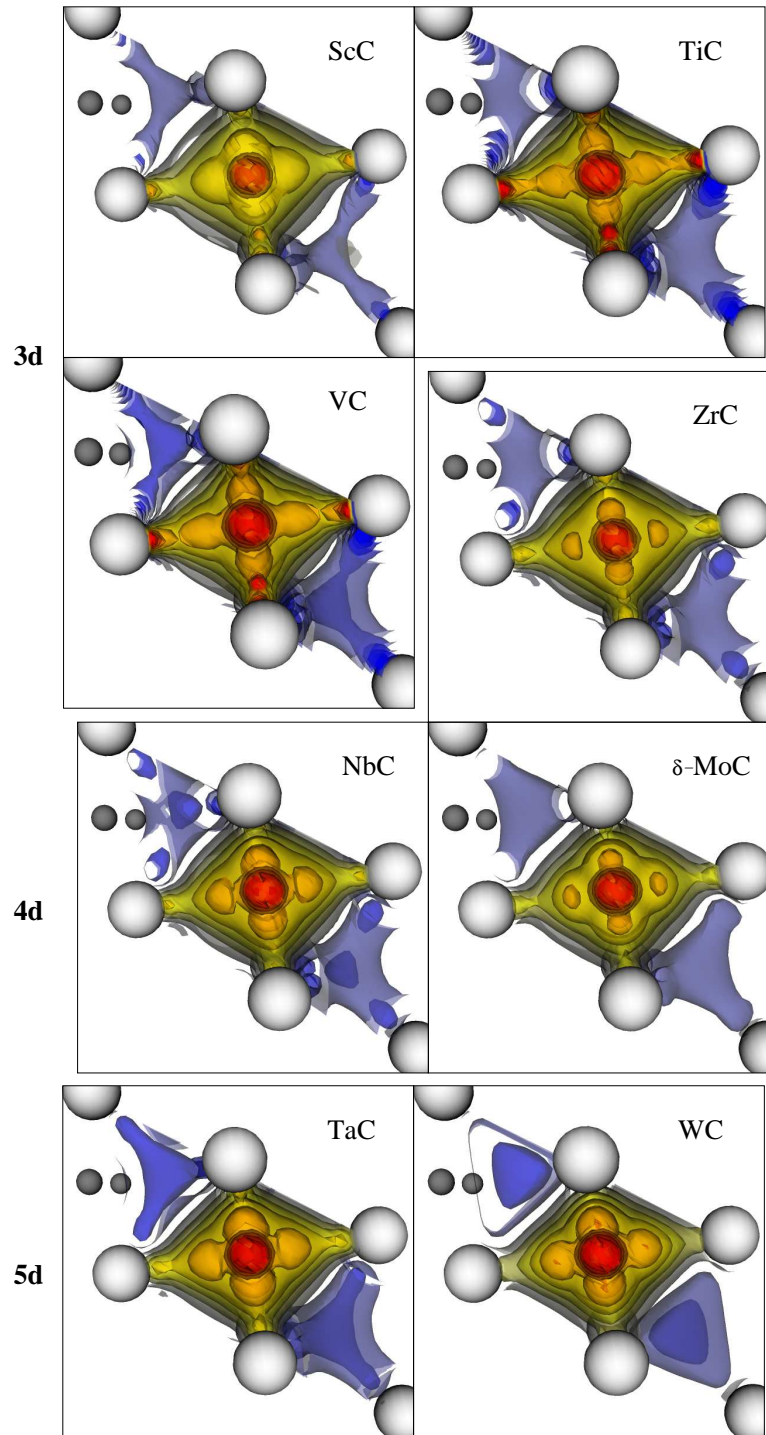


FIG. 4: Valence-electron density difference plots for the considered bulk systems, compared to the free constituent TM and C atoms. The structures are viewed along the [111] direction. Twenty isosurfaces homogeneously distributed in the interval $[-0.4, 0.5]$ electrons/ \AA^3 are shown. The color coding is blue (reduction of electron density) through yellow (no density difference) to red (increase in electron density). Larger (gray) balls correspond to TM atoms and smaller black balls are C atoms. The atom situated in the central red region is C.

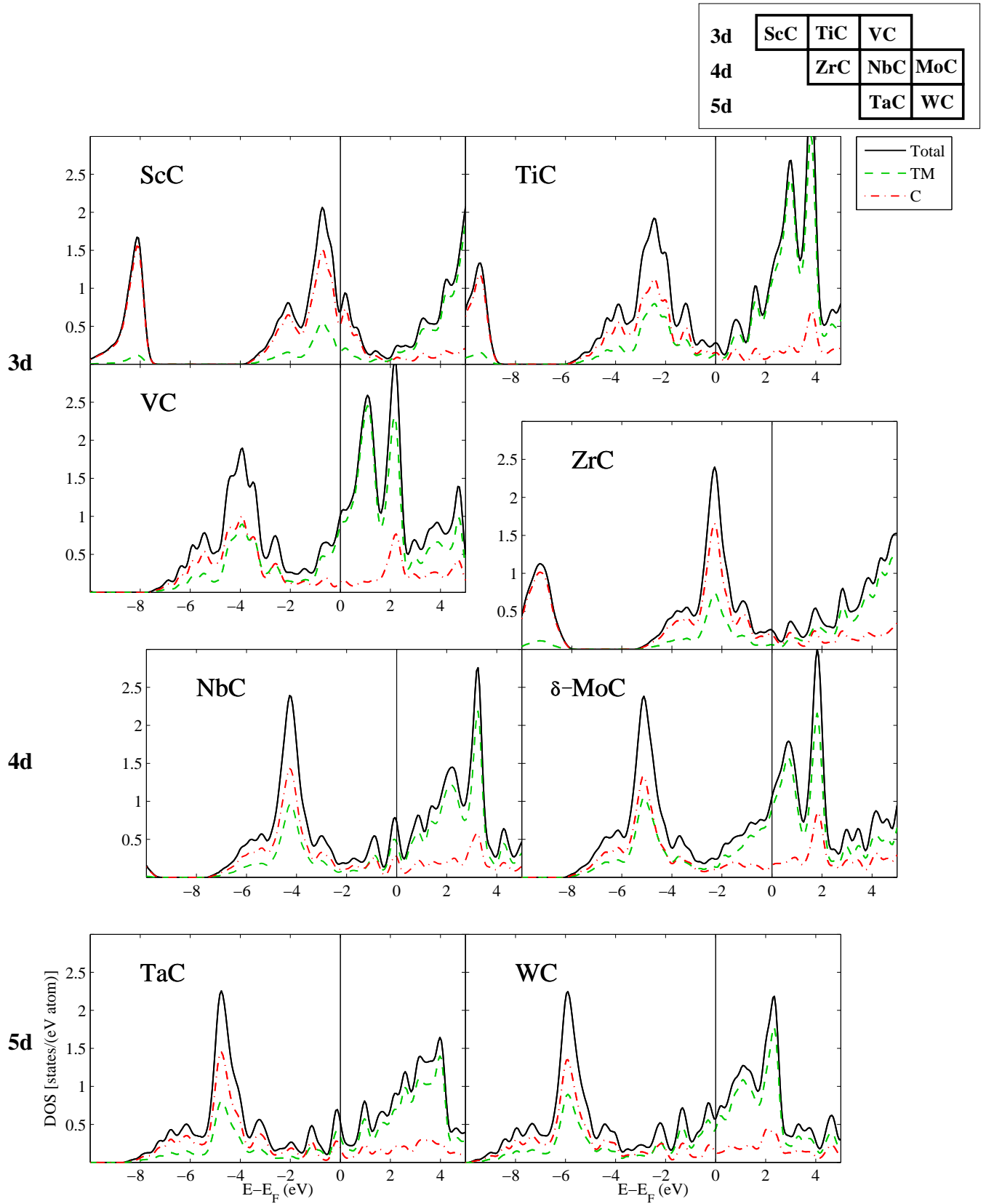


FIG. 5: Total and atom-projected densities of states for the considered bulk transition-metal carbide systems.

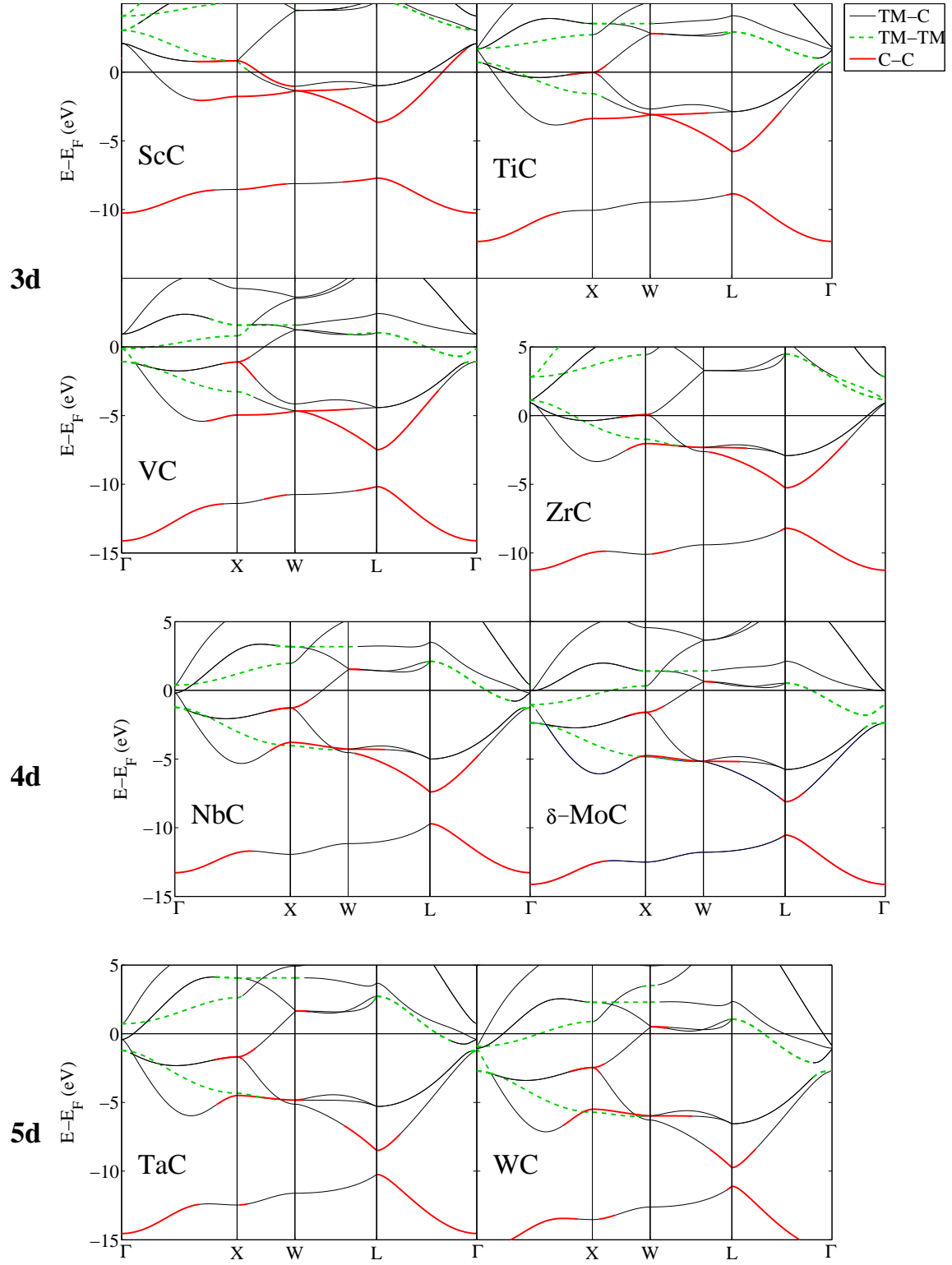


FIG. 6: Calculated band structures for the considered TMC's. The parts of the bands that correspond to TM-TM, TM-C and C-C bonding states, respectively, are indicated. The identification of the bond character is based on the Kohn-Sham wave functions as described in the text and visualized in Fig. 7.

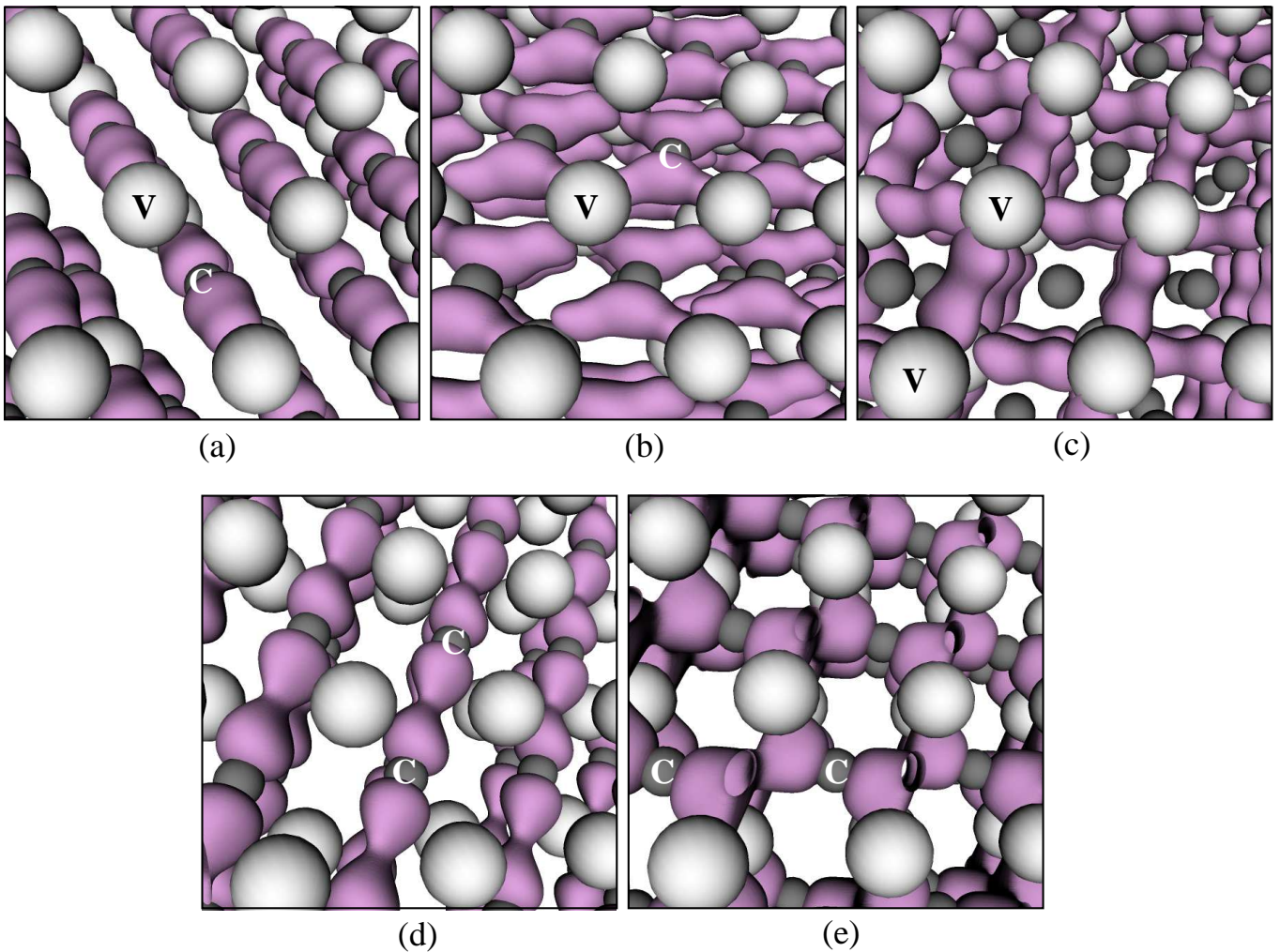


FIG. 7: Three-dimensional real-space contour plots of a representative selection of the Kohn-Sham wave functions $|\Psi_{n\mathbf{k}}(\mathbf{r})|$ in bulk VC illustrating the different types of bonds at specific \mathbf{k} points and bands n (here, $n = 1$ corresponds to the lowest valence band, cf. Fig. 6): (a) $\text{TM}(t_{2g})\text{-C}(p)$ σ bonds found in the lowest UVB band ($n = 2$) between Γ and X , (b) $\text{TM}(e_g)\text{-C}(p)$ π bonds at $L_{n=3}$, (c) $\text{TM}(t_{2g})\text{-TM}(t_{2g})$ σ at $X_{n=3}$, (d) $\text{C}(p)\text{-C}(p)$ σ at $W_{n=2}$, (e) $\text{C}(p)\text{-C}(p)$ π at $L_{n=2}$ (there is no connection to the V atoms). The given contour plots are for the same value of $|\Psi_{n\mathbf{k}}(\mathbf{r})| = 0.30$. Larger (gray) balls correspond to V atoms and smaller black balls ones to C atoms.

a filled (or, for ScC, partly filled) bonding upper valence band (UVB) below E_F , with overlapping C $2p$ and TM d states; (iii) an empty or partly filled antibonding conduction band (CB) above or around E_F , dominated by TM d states with a clear contribution from C $2p$ states; and (iv) a non-vanishing DOS in the pseudogap between the UVB and the CB.

The contribution to the bonding from the LVB is presumably small due to the small hybridization of the TM and C states. Points (ii) and (iii) illustrate the presence of a covalent bond. The mainly C $2p$ and TM d characters of the UVB and CB, respectively, indicate a partially ionic bonding nature. Orbital-projected DOS's show that the TM states are of predominantly e_g and t_{2g} symmetry in the UVB and in the CB, respectively. Property (iv) explains the metallic character of the TMC's.

An analysis of the Kohn-Sham wave functions along

the k symmetry lines of Fig. 6 shows that the band structure is dominated by TM-C states [see Figs. 7(a)-(b) for representative TM-C bonds in the case of VC]. These states are found throughout the whole energy region of the k space, that is, they are present in both the LVB and the UVB, as well as in the CB.

The wave function analysis reveals also that large parts of the states in the LVB and in the lower energy range of the UVB have a bonding C-C character of both σ and π symmetry [see Figs. 7(d)-(e) for representative C-C bonds in the case of bulk VC].

Finally, TM-TM states are evident in significant parts of both the UVB and the CB [see Fig. 7(c) for a representative TM-TM bond in the VC system]. In all the TMC's, at least one band of TM-TM character crosses E_F .

The wave function analysis confirms also the picture

that the UVB states have a bonding symmetry, while the CB states show a more antibonding character (*i.e.*, nodes in between the atoms).

Experiments on the band structures for single bulk crystals of group IV-VI TMC's have been carried out by using, for example, angle-resolved photo-emission spectroscopy (ARPES), in particular X-ray photoemission spectroscopy (XPS) for the mapping of occupied bands and inverse photo-emission spectroscopy (IPES) for the mapping of unoccupied bands (see Ref. 21 and references therein). These results agree with the rough features of our calculated results but do not provide any information on the different bond characters of the different bands, which our method is able to give.

2. Trends along a period

The DOS figures, together with the band structure and wave function analyses, show that, as the TM group number increases, (i) both the UVB and the CB (as well as the LVB) are shifted down in energy relative to E_F , due to the filling of bands; (ii) as a consequence the metallicity (*i.e.*, the number of states at E_F) increases; (iii) the bands crossing E_F show more TM-TM character; (iv) the energy separation between the UVB and the CB decreases; (v) the UVB becomes less C localized; and (vi) the overall amount of C-C states decreases.

3. Trends along a group

As the TM period number increases the following general features are observed in the DOS, band structure, and wave function plots: (i) the position of E_F relative to the center of mass of the UVB and the CB is unchanged; (ii) the bond character of the different states is largely unchanged; (iii) the energy separation between the UVB and the CB increases; and (iv) the UVB becomes more C localized. The differences between periods 5 and 6 are smaller than the differences between periods 4 and 5.

Also, a detailed investigation of the band structure reveals that the energetical order of the bands changes: (i) at the Γ point the higher TM-TM band moves up in energy, while TM-C bands move down; and (ii) the two lowest UVB bands at the X point (the C-C and the TM-TM bands) approach each other and change places.

D. Understanding the trends

The above trends can be explained on the basis of a two-level system, comprised of the valence d and p states of the free TM and C atoms, respectively (see Fig. 8). This discussion resembles the one for a heteronuclear diatomic molecule (see for example Ref. 37). Due to the lower electronegativity of the TM atom, the energy of the TM d state is higher than that of the C p state.

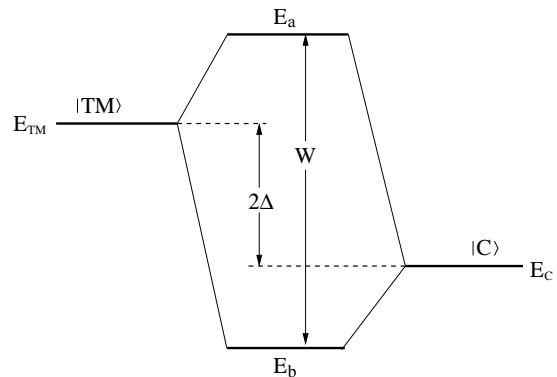


FIG. 8: An illustration of a two-level system consisting of the valence TM and C states. The bonding E_b and antibonding E_a states correspond to the UVB and CB of the TMC, respectively.

Their interaction results in bonding E_b and antibonding E_a states, the UVB and the CB, respectively, separated by an energy W (see Fig. 8). Assuming a one-electron picture, the solutions to the Schrödinger equation are

$$E_b = \varepsilon - \sqrt{\Delta^2 + \beta^2} \quad (2)$$

$$E_a = \varepsilon + \sqrt{\Delta^2 + \beta^2}, \quad (3)$$

with $\varepsilon = (E_{TM} + E_C)/2$ and $\Delta = (E_{TM} - E_C)/2$, where E_{TM} is the energy of the TM d level and E_C is the energy of the C p level, and $\beta = \langle C|H_{12}|TM\rangle$. If $\Delta \neq 0$, which is the case here, there is a charge transfer from TM to C and the bond is partially ionic.

As the TM group number increases, the TM level is shifted down in energy, due to the increase of d electrons, giving a better energy overlap between the TM and C states. This results in a stronger pd hybridization, a smaller Δ , and a bond of more covalent character, that is, a more similar amount of TM and C localization of the UVB. At the same time, the increase of d electrons causes a shift of E_F towards higher energies. The separation between UVB and CB is given by $W = 2(\Delta^2 + \beta^2)^{1/2}$. Along a period, each extra d electron is added in the same valence shell. To a first approximation one can therefore assume that β is constant along a period. Hence, W becomes smaller, which is confirmed by our DFT calculations (see Fig. 5).

Moving down a group, the number of d electrons is constant, leaving E_F at the same energy. However, the TM level is shifted up in energy, resulting in a smaller pd hybridization and a larger separation between the TM and the C levels, giving a more ionic bond. As the separation increases, the closer the resulting levels come to the original ones, giving them more character of the original levels, that is, the UVB (CB) becomes more C (TM)-localized.

This picture is supported by our calculated Bader charge-transfer trends (Table I). To the right along a period, the ionicity decreases, which results in decreasing Bader values (except for δ -MoC, as mentioned in

Sec. III B). Down a group, the increase in ionicity is reflected by increasing Bader values.

IV. DISCUSSION

In this paper we present a systematic and detailed trend study of the electronic structure of a collection of early transition-metal carbides based on DFT calculations.

The results confirm the mixed ionic-covalent TM–C and the metallic TM–TM nature of the bond. This is shown both by local DOS analyses and by a thorough analysis of the band structures and Kohn-Sham wave functions along several symmetry lines in the Brillouin zone (Fig. 6). TM–C bands are present throughout the whole energy range of the k space, including the pseudogap between the UVB and the CB. Also, both a bonding and an antibonding TM–TM band are identified.

In addition, our analysis shows that in all the considered TMC's there exist direct C–C bonds, localized mainly in the lower part of the UVB. This presence is most pronounced in ScC (where C–C bands cross E_F) and decreases as the TM group and period numbers increase. The C–C bonds are also found in the pseudogap.

Hence, the C atoms play two roles for the bonding in the TMC's, by their interaction with the TM atoms and with other C atoms, respectively.

The valence-electron density difference analysis shows that the dominating bond character is the ionic-covalent TM–C bond, which is supported by the mapping of bands in the band structure (see Fig. 6). The trends in the covalent and ionic contributions can be extracted even though these two bonding types are closely intertwined. We find that the covalent contribution increases from left to right along a period and decreases down a group, while the ionic one decreases from left to right and increases down a group. In addition, our results show that there is a correlation between the covalency and the separation between the UVB and CB. A larger covalency corresponds to a larger separation.

Although the TM–TM and C–C bonds are not observed in the density difference plots, their existence is revealed by the real-space wave function analysis. A contribution from C–C bonds to the TMC cohesion has been suggested in Ref. 14 based on a two-sublattice model. However, such a model does not take into account the modifying effect of the TM d states on the C orbitals in the C sublattice, and vice versa. Our approach identifies the different bonding types directly from the calculated electronic structure and therefore includes this modifying effect. We find that a significant amount of C–C states are present in all the studied TMC's, that is, not only the metastable ones, as was suggested in Ref. 14.

All the studied TMC's have a metallic bond character, that is, a non-vanishing DOS at E_F . These states (Fig. 6) are of both TM–TM and TM–C character (for ScC also C–C states). Indeed, measurements show that group IV

and V TMC's are almost as good electrical conductors as the parent metals.⁹ With an increasing DOS at E_F (Fig. 5), and assuming everything else weakly varying, the conductivity should increase from group IV to group VI, which agrees with measurements.⁹ On the same arguments, the conductivity of ScC should be comparable to that of VC.

As discussed in Sec. III A, along a period the calculated cohesive energies exhibit a maximum for group IV. The calculated electronic structure shows that for group IV, E_F is positioned in the pseudogap between the UVB and the CB, meaning that all the bonding UVB states are filled and all the antibonding CB states are empty. The same arguments as in the case of the bonding energy in a diatomic molecule can be applied, that is, a filling of bonding states increases the bond strength, while filling of antibonding states reduces the bond strength.^{10–12,15,20} For ScC, not all bonding UVB states are filled and therefore the cohesive energy is lower for this compound. For groups V and VI, the antibonding CB states are partly filled, which again results in a weaker bond.

Down a group, the cohesive energies of the TMC's increase. This is because the UVB is shifted down in energy, making the bond stronger, while the CB is shifted up in energy, resulting in an energy gain due to the emptying of antibonding states.

The band structure and Kohn-Sham wave function analyses show the origin of the instability of MoC and WC in NaCl structure. The instability arises from the filling of antibonding states, as shown in Fig. 6. In MoC, the TM–TM antibonding band around Γ is partly filled. In WC, two additional antibonding bands, of W–C character, cross E_F around the Γ point and become partly occupied. This picture agrees with previous studies¹³ but also provides additional details.

The detailed analysis of the electronic structure provided in this study lays the essential foundation for the understanding of the TMC's surface properties, such as their surface reactivity. The surface characteristics of a material are tightly bound to its underlying bulk properties, and will of course depend strongly on the type of bonds that are broken upon creation of the surface. It is, for example, known that the surface electronic structure of the TMC (100) surfaces is similar to that of the bulk. However, the TMC (111) surface shows both TM-localized as well as C-localized surface resonances.^{1,5,6} The importance of these resonances on the surface reactivity is investigated in Refs. 5 and 6.

V. CONCLUSIONS

This trend study deals with the bonding nature of early TMC's. Our approach is based on a complementary use of different types of electronic-structure analysis tools. In particular, a thorough mapping of the band structure provides detailed insight into the bonding of

the bulk TMC's. The results (i) confirm that the dominant contribution to the bond is the ionic-covalent TM-C bond, (ii) show the existence of TM-TM bonds, and, importantly, (iii) reveal the existence of direct C-C bonds (most pronounced for ScC). We provide new information on the spatial extent of the different bonds, on their k -space location within the band structure, and on their importance for the bulk cohesion. Also, trends in covalency *vs.* ionicity are obtained. The resulting electron-structural trends are analyzed and discussed within a two-level model.

These results are of importance for the understanding of the TMC surface reactivities, due to the intimate relation between bulk and surface electronic structures. When creating a surface by cutting a crystal, the break-

ing of TM-C, TM-TM, and C-C bonds can manifest themselves as surface resonances and/or surface states at the surface. As we show in another study, not only TM but also C resonances play a crucial role in the bonding mechanism on TMC surfaces.^{5,6}

Acknowledgments

The authors thank B. I. Lundqvist and A. Hellman for reading the manuscript and for providing valuable suggestions. Allocation of computer time via SNIC (Swedish National Infrastructure for Computing) is gratefully acknowledged.

* Electronic address: alevoj@chalmers.se

- ¹ C. Ruberto, and B. I. Lundqvist, Phys. Rev. B **75**, 235438 (2007).
- ² A. Vojvodic, C. Ruberto and B. I. Lundqvist, Surf. Sci. **600**, 3619 (2006).
- ³ C. Ruberto, A. Vojvodic and B. I. Lundqvist, Surf. Sci. **600**, 1612 (2006)
- ⁴ C. Ruberto, A. Vojvodic and B. I. Lundqvist, Solid State Commun. **141**, 48 (2007).
- ⁵ A. Vojvodic, A. Hellman, C. Ruberto and B. I. Lundqvist, submitted.
- ⁶ A. Vojvodic, C. Ruberto and B. I. Lundqvist, in preparation.
- ⁷ T. Bligaard and J. K. Nørskov, in *Chemical Bonding at Surfaces and Interfaces*, edited by A. Nilsson, L. G. M. Pettersson, and J. K. Nørskov, (Elsevier, Amsterdam, 2008).
- ⁸ S. T. Oyama, editor, *The Chemistry of Transition Metal Carbides and Nitrides* (Blackie Academic and Professional, London, 1996).
- ⁹ H. O. Pierson, *Handbook of refractory carbides and nitrides: properties, characterisation, processing and applications* (Noyes Publications, Westwood, New Jersey, USA, 1996).
- ¹⁰ A. Neckel, P. Rastl, R. Eibler, P. Weinberger, and K. Schwarz, J. Phys. C: Solid State Phys. **9**, 579 (1976).
- ¹¹ K. Schwarz, CRC Crit. Rev. Sol. St. Mater. Sci. **13**, 211 (1987).
- ¹² V. P. Zhukov, V. A. Gubanov, O. Jepsen, N. E. Christensen, and O. K. Andersen, J. Phys. Chem. Solids **49**, 841 (1988).
- ¹³ D. L. Price, and B. R. Cooper, Phys. Rev. B **39**, 4945 (1989).
- ¹⁴ Y. Zhang, J. Liu, L. Zhou and S. Xiang, Solid State Commun. **121**, 411 (2002).
- ¹⁵ C. D. Gelatt, A. R. Williams, and V. L. Moruzzi, Phys. Rev. B **27**, 2005 (1983).
- ¹⁶ A. F. Guillermet, and G. Grimvall, Phys. Rev. B **40**, 10582 (1989).
- ¹⁷ J. Häglund, G. Grimvall, T. Jarlborg, A. F. Guillermet, Phys. Rev. B **43**, 14400 (1991).
- ¹⁸ A. Fernández Guillermet, J. Häglund, G. Grimvall, Phys. Rev. B **45**, 11557 (1992).
- ¹⁹ A. F. Guillermet, J. Häglund, G. Grimvall, Phys. Rev. B **48**, 11673 (1993).
- ²⁰ J. Häglund, A. Fernández Guillermet, G. Grimvall, and M. Körling, Phys. Rev. B **48**, 11685 (1993).
- ²¹ L. I. Johansson, Surf. Sci. Rep. **21**, 177 (1995).
- ²² J. C. Grossman, A. Mizel, M. Côté, M. L. Cohen, and S. G. Louie, Phys. Rev. B **60**, 6343 (1999).
- ²³ F. Viñes, C. Sousa, P. Liu, J. A. Rodriguez, and F. Illas, J. Chem. Phys. **122**, 174709 (2005).
- ²⁴ T. Das, S. Deb, and A. Mookerjee, Physica B **367**, 6 (2005).
- ²⁵ <http://wiki.fysik.dtu.dk/dacapo>
- ²⁶ D. Vanderbilt, Phys. Rev. B **41**, 7892 (1990).
- ²⁷ K. Burke, J. P. Perdew, and Y. Wang, in *Electronic Density Functional Theory, Recent Progress and New Directions*, edited by J. F. Dobson, G. Vignale and M. P. Das (Plenum Press, New York and London 1998), pp. 81–111.
- ²⁸ H. J. Monkhorst and J. D. Pack, Phys. Rev. B **13**, 5188 (1976).
- ²⁹ F. D. Murnaghan, Proc. Natn. Acad. Sci. **30**, 244 (1944).
- ³⁰ R. F. W. Bader, Chem. Rev. **59**, 893 (1991).
- ³¹ G. Henkelman, A. Arnoldsson and H. Jonsson, Comp. Mat. Sci. **36**, 354 (2006).
- ³² K. Nakamura, and M. Yashima, Materials Science and Engineering B, **148** 69 (2005).
- ³³ Z. Dridi, B. Bouhafs, P. Ruterana and H. Aourag, J. Phys.: Condens. Matter **14** (1995).
- ³⁴ B. Cordero, V. Gómez, A. E. Platero-Prats, M. Revés, J. Escheverría, E. Cremades, F. Barragán, and S. Alvarez, Dalton Trans. **21**, 2832 (2008).
- ³⁵ R. D. Shannon, Acta Crystallogr. **A32**, 751 (1976).
- ³⁶ J. G. Chen, Surf. Sci. Rep. **30**, 1 (1997).
- ³⁷ A. P. Sutton, *Electronic Structure of Materials*, (Oxford Science Publication, New York, United States, 1994).